INTERNATIONAL JOURNAL FOR NUMERICAL AND ANALYTICAL METHODS IN GEOMECHANICS, VOL. 12, 141–155 (1988)

MODELLING AND SIMULATION OF LOAD TRANSFER IN REINFORCED SOILS: PART 1

I. JURAN[†], A. GUERMAZI[‡], C. L. CHEN[§] AND M. H. IDER[§]

Department of Civil Engineering, Louisiana State University, Baton Rouge, LA 70803, U.S.A.

SUMMARY

Results of both triaxial and direct shear tests on reinforced soil samples performed by different investigators have shown that soil dilatancy and extensibility of the reinforcements have a significant effect on the generated tension forces in the inclusions. An appropriate soil–reinforcement load transfer model, integrating the effect of soil dilatancy and reinforcement extensibility is therefore needed to adequately predict forces in the inclusions under expected working loads. This paper presents a load transfer model assuming an elasto-plastic strain hardening behaviour for the soil and an elastic–perfectly plastic behaviour for the reinforcement. This model is used to analyse the response of the reinforced soil material under triaxial compression loading. A companion paper presents the application of this model for numerical simulations of direct shear tests on sand samples reinforced with different types of tension resisting reinforcements. The model allows an evaluation of the effect of various parameters such as mechanical characteristics and dilatancy properties of the soil, extensibility of the reinforcements, and their inclination with respect to the failure surface, on the development of resisting tensile stresses in the reinforcements. A parametric study is conducted to evaluate the effect of these parameters on the behaviour of the reinforced soil material. An attempt is also made to verify the proposed model by comparing numerical predictions with available experimental results of both triaxial and direct shear tests on reinforced soil samples. This model can be used for analysis and design of reinforced soil walls with different types of tension resisting inclusions to predict tension forces under expected working loads.

INTRODUCTION

Over the past two decades, the techniques of soil reinforcement have been increasingly used in the construction of embankments, retaining walls and bridge abutments. In this context, new systems using different types of reinforcing materials have developed. However, in spite of the accumulation of construction experience, the design methods used at present are still essentially based either on limit equilibrium analyses or on semi-empirical methods that often consider over-simplified assumptions. Specifically, these design methods do not properly account for the realistic stress–strain properties of the reinforcement and the soil, which can significantly affect the tension forces in the inclusions of actual reinforced soil structures.

The rapidly increasing use of a large variety of extensible reinforcements such as geotextiles and geogrids requires appropriate strain compatibility design methods to predict tension strains and stresses in the inclusions under expected working loads. A rational modelling of the complex load

[†] Associate Professor.
[‡] Research Associate.
[§] Graduate Student.

0363–9061/88/020141–15$07.50

Received 6 April 1987
Revised 11 June 1987

transfer mechanism in the reinforced soil mass is therefore needed in order to evaluate and integrate in design the effect of various parameters. Some of these parameters are: extensibility of the inclusion, mechanical characteristics and dilatancy properties of the soil, and inclination of the reinforcement with respect to the potential failure surface.

In recent years, a few researchers have conducted laboratory studies to investigate the behaviour of the reinforced soil material under different types of loading paths. These studies include triaxial tests on sand specimens reinforced by a variety of inclusions, such as aluminium foils, [1-3] fibreglass grids[4] and fabrics,[5] as well as direct shear tests on sand specimens reinforced by geotextiles or geogrids.[6-11]

Analyses of the test results have been mainly focussed on evaluating the reinforcement effect on the shear strength characteristics of the composite reinforced soil material. Two apparently different definitions have been proposed to formulate an equivalent failure criterion by considering: (1) an 'equivalent extension restraint–confining stress' concept,[4] and (2) a 'pseudo-cohesion' concept.[1] These failure criteria consider an equivalent, anisotropic 'homogenized' material with global shear strength characteristics which are related to the intrinsic soil properties and to the ultimate tension forces in the inclusions using limit equilibrium equations. The ultimate tension forces are equal to either the tensile or the pull-out resistance of the inclusion.

Results of both triaxial test[2] and direct shear tests[8-11] on sand samples reinforced with tensile inclusions have shown that the apparent cohesion of the reinforced soil material is a function of the orientation of the inclusions with respect to the direction of the maximum extension in the soil. Specifically, the results of the direct shear tests have illustrated that forces in the inclusions can be either tensile or compressive depending upon their inclination with respect to the failure surface and the dilatancy rate of the soil.

The effect of the dilatancy rate of the sand on the forces generated in the inclusions was investigated by Jewell[8] and Dyer and Milligan.[10] They used X-ray radiographic technique to measure the displacement field in the soil around the inclusion in the reinforced soil sample. The results of their analyses illustrate that the increase of tension forces in the inclusion can be reasonably related to the measured extension rate of the sand in the direction of the inclusion assuming a perfect soil–inclusion adherence. These results also indicate that soil dilatancy has a significant role in the load transfer from the soil to the inclusion. An appropriate load transfer model is therefore required in order to evaluate the effect of soil dilatancy on tension forces generated in the inclusions. Such a model should also allow an integration in design of nonlinear stress–strain relationships of the reinforcements.

The purpose of this study is to develop a load transfer model capable of simulating the response of the reinforced soil material to different stress paths, specifically: (1) triaxial compression test, and (2) simple shear test. This paper presents the modelling assumptions, the predicted effect of the various parameters on the behaviour of the reinforced soil material and an attempt to verify the proposed model by comparing numerical test simulations with experimental results of triaxial tests on reinforced soil samples. A companion paper presents the application of this model to numerical simulations of direct shear tests on sand samples reinforced with different types of tension-resisting inclusions.

MODELLING ASSUMPTION

Modelling the behaviour of a reinforced soil material requires:

1. An appropriate constitutive equation for the soil capable of representing incrementally the strain path at any point of the soil mass including soil–reinforcement interfaces.

2. A stress–strain relationship for the reinforcing material.
3. A rational but simple assumption concerning soil–reinforcement interaction.

Reinforcement

Behaviour of reinforcement is assumed to be an isotropic, elastic–perfectly plastic material and its stress–strain relationship is written as

$$d\sigma_R = E\,d\varepsilon_R \quad \text{with} \quad \sigma_R \leq R_T \tag{1}$$

where σ_R and ε_R are, respectively, the tensile stress and strain in the reinforcement, E is the elastic modulus, and R_T is the tensile resistance (or elastic limit) or pull-out resistance of the reinforcement, whichever is smaller. Nonlinearity of the stress–strain relationship of the reinforcement can be considered by introducing an elastic modulus $E(\varepsilon_R)$ as a function of the strain level.

Sand

For behaviour of sand the elasto-plastic model used[12] considers the soil to be homogeneous, isotropic, and strain hardening material with a non-associated flow rule. Here, elastic strains during shearing are neglected.

Yield function. A Mohr–Coulomb type yield criterion is considered to define the yield surface with an open elastic domain. The assumed yield function can be written as

$$F(\sigma_{ij}, x) = t/s - h(x) = 0 \tag{2}$$

where σ_{ij} is the stress tensor, $t = (\sigma_1 - \sigma_3)/2$ is the deviatoric stress, $s = (\sigma_1 + \sigma_3)/2$ is the average stress, σ_1 and σ_3 are the major and the minor principal stresses, respectively, x is the strain hardening parameter and $h(x)$ is the strain hardening (and post-peak strain softening) function which relates the actual yield surface to the current state of strain.

The strain hardening and post-peak strain softening is assumed to be isotropic. The strain hardening parameter is defined by the shear strain: $x = \gamma = \varepsilon_1 - \varepsilon_3$, where ε_1 and ε_3 are the principal strains with $\varepsilon_1 > \varepsilon_3$.

For the rotational stress path applied in the simple (or direct) shear test, it is more convenient to consider as a strain hardening parameter the applied shear strain ($x = \gamma_{xy}$). The Mohr–Coulomb's type yield function can then be written as

$$F(\sigma_{ij}, \gamma_{xy}) = \tau_{xy}/\sigma_y - g(\gamma_{xy}) = 0 \tag{3}$$

where τ_{xy} and σ_y are, respectively, the applied shear and normal stresses, and the $g(\gamma_{xy})$ function is related to the $h(x)$ function by the uniqueness of the assumed yield function.

Figures 1(a) and 1(b) show schematically the strain hardening function $h(x)$ and associated volumetric strains for both loose contracting and dense dilating sands.

For loose contracting sands, it is assumed that $h(x)$ is a hyperbolic function which can be written as

$$h(x) = x/(a + bx) \tag{4a}$$

with

For triaxial test: $1/a = G/\sigma_0$; $1/b = \sin \phi_{cv}$
For direct (or simple) shear test: $1/a = G/\sigma_0$; $1/b = \tan \phi_{cv}$

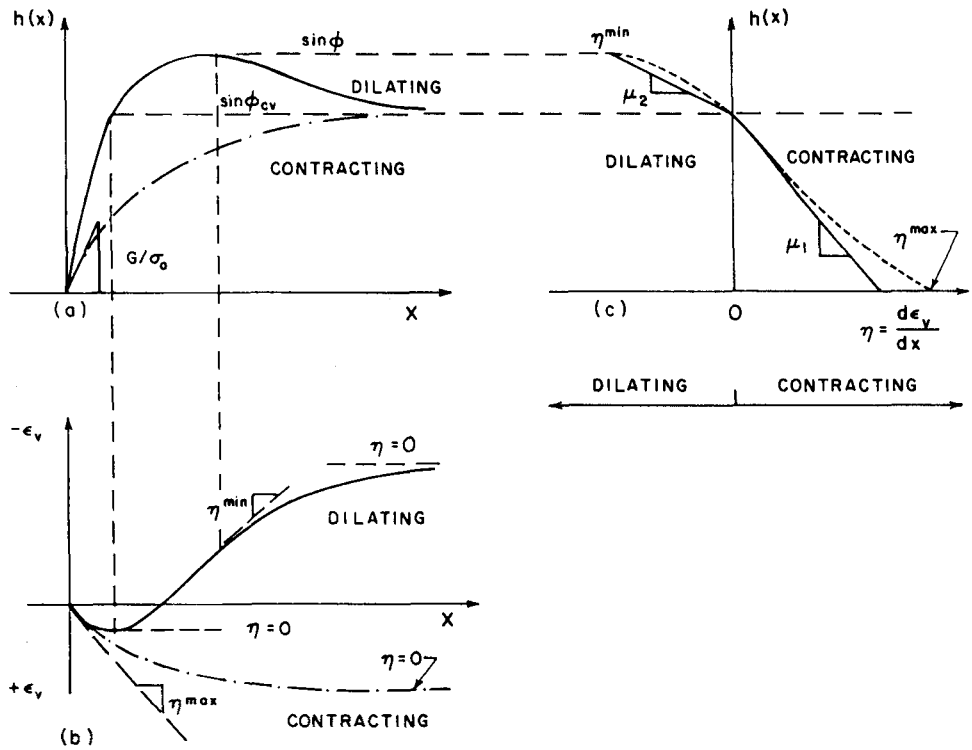

Figure 1. Assumed constitutive equations and related soil parameters

where σ_0 is the initial isotropic consolidation stress applied in the triaxial test and σ_y is the normal stress applied in the direct (or simple) shear test, G is the initial shear modulus, and ϕ_{cv} is the critical state friction angle of the soil.

For dense dilating sands, it is assumed that the hardening function $h(x)$ is a parabolic function and can be written as

$$h(x) = cx(x-a)/(x+b)^2 \tag{4b}$$

where the constants a, b and c are determined from the following conditions, for triaxial test: (1) the initial tangent modulus of the $h(x)$ function is equal to G/σ_0, (2) at the peak stress ratio $h(x) = \sin\phi$, and (3) at the critical state, $h(x) = \sin\phi_{cv}$, these conditions yield

$$c = \sin\phi_{cv}$$
$$a = -4(\sigma_0/G)[\sin^2\phi \cdot l^2]/\sin\phi_{cv}$$
$$b = 2(\sigma_0/G)[\sin\phi \cdot l]$$

with $l = 1 + [1 - (\sin\phi_{cv}/\sin\phi)]^{1/2}$. For a direct shear test, replace σ_0 by σ_y, and $\sin\phi$ and $\sin\phi_{cv}$, respectively, by $\tan\phi$ and $\tan\phi_{cv}$ to obtain the corresponding strain hardening function $g(\gamma_{xy})$.

The plastic flow of the sand in direct (or simple) shear tests has been investigated by different authors.[13-16] They showed that the plastic energy dissipated in the material during simple shearing is proportional approximately to the applied normal stress and therefore energy

considerations lead to a linear stress ratio–dilatancy function which can be written as

$$\frac{\tau_{xy}}{\sigma_y}+\frac{d\varepsilon_y}{d\gamma_{xy}}=c=\tan\phi_{cv} \tag{5a}$$

where $d\varepsilon_y$ is the soil extension (or compression) increment in a direction orthogonal to the failure surface.

A correction modulus μ_s is introduced to obtain a more realistic stress ratio–dilatancy function which can be approximated by a bilinear curve as

$$\tan\nu=\frac{d\varepsilon_y}{d\gamma_{xy}}=\frac{1}{\mu_s}\left[\tan\phi_{cv}-\frac{\tau_{xy}}{\sigma_y}\right] \tag{5b}$$

with

$\mu_s=\mu_1$ when $\tau_{xy}/\sigma_y\leq\tan\phi_{cv}$ – contracting behaviour

$\mu_s=\mu_2$ when $\tau_{xy}/\sigma_y>\tan\phi_{cv}$ – dilating behaviour

and ν is the dilatancy angle.

It is assumed that a unique relationship, independent of the actual stress path, exists between the stress ratio q/p and the dilatancy rate $\eta=d\varepsilon_v/d\gamma$. Therefore, for a triaxial stress path, the stress ratio–dilatancy function can be written as

$$\eta=\frac{1}{\mu_T}[\sin\phi_{cv}-t/s] \tag{6a}$$

where the correction modulus μ_T is related to μ_s by the uniqueness of the $\eta(t/s)$ function.

Equation (6a) may be rewritten in terms of stress invariants (q, p) as

$$\frac{d\varepsilon_v}{d\gamma}=\frac{1}{\mu}[M_{\phi_{cv}}-q/p] \tag{6b}$$

where

$$q=\sigma_1-\sigma_3$$

$$p=1/3(\sigma_1+2\sigma_3)$$

$$M_{\phi_{cv}}=\frac{6\sin\phi_{cv}}{3-\sin\phi_{cv}}$$

A non-associated plastic potential function $Q(q/p)=0$ can then be derived. Assuming coincidence of principal axes of stresses and plastic strain increments, the normality condition (i.e. the plastic strain increment vector is normal at any point to the surface $Q(q, p)=0$) implies that, as elastic strains are neglected,

$$\frac{dq}{dp}=-\frac{d\varepsilon_v^p}{d\gamma^p}=-\frac{d\varepsilon_v}{d\gamma} \tag{7a}$$

Substituting expression (7a) into equation (6b) and integrating, we obtain the plastic potential function which can be written as

$$Q(p, q)=\frac{q}{p}-\frac{M_{\phi_{cv}}}{1-\mu}\left[1-\mu\left(\frac{p}{p_0}\right)^{((1-\mu)/\mu)}\right]=0 \tag{7b}$$

where p_0 is the isotropic stress at the intersection of the projection of the plastic potential surface in

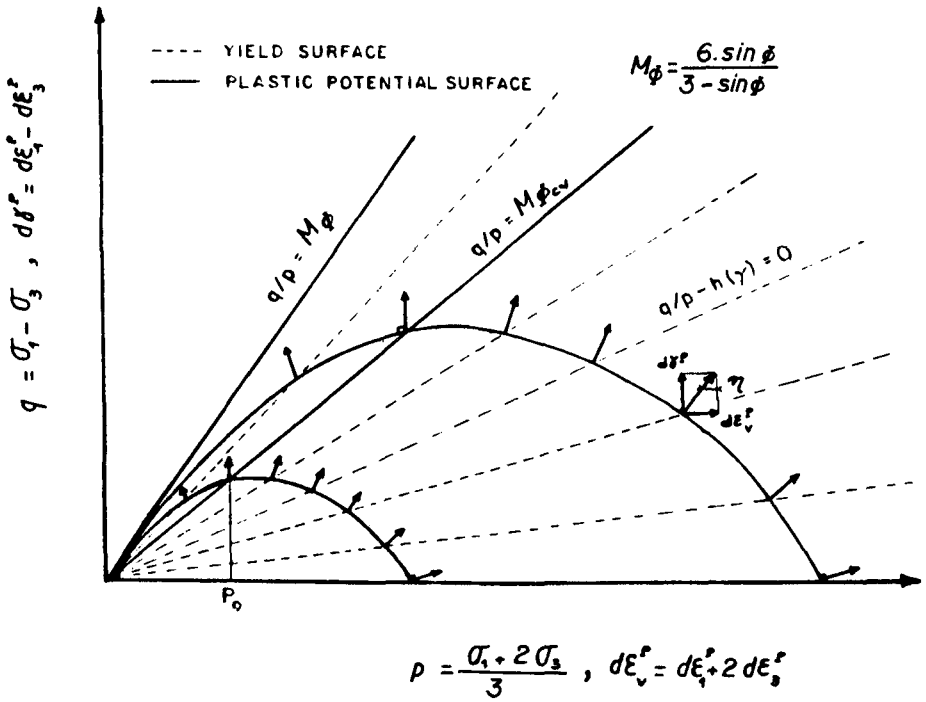

Figure 2. Yield and plastic potential surfaces

the (q, p) plane with the critical state line. The projection of the assumed yield surface and plastic potential surface in the (q, p) plane are illustrated in Figure 2.

Figure 1(c) shows schematically the stress ratio–dilatancy rate $\eta(q/p)$ functions for both contracting loose and dilating dense sands. The maximum plastic dilatancy rate $\eta^{\min} = \min(d\varepsilon_v/dx)$ is approximately equal to the slope of the volumetric strain–shear curve at the peak of the $h(x)$ function, whereas the dilatancy rate at the residual critical state is equal to $\eta = 0$.

The proposed soil model requires five parameters: G/σ_0 or (G/σ_y), ϕ, ϕ_{cv}, μ_1 and μ_2 (or $\eta^{\min}$) which, as illustrated in Figures 1(a) and 1(c), can be determined from the analysis of either conventional triaxial test or direct shear test results. It should be indicated that these sand characteristics are dependent on the applied confining pressure and initial relative density. Therefore, average characteristics of a sand compacted to a given relative density are used to represent its behaviour in each specified range of confining stresses.

SOIL–REINFORCEMENT INTERACTION

The mechanism governing soil–reinforcement interaction in a reinforced soil mass has already been the object of both experimental and theoretical studies. The concept is relatively simple.[17] As a reinforced soil sample is axially loaded in the triaxial test, the soil tends to expand laterally. The friction mobilized at the interfaces restrains the relative displacement between the two ingredients of the reinforced soil sample. Consequently, the lateral expansion of the sample is governed by the extensibility (or elastic modulus) of the reinforcements. The mobilized soil–reinforcement friction

causes a build-up of the tensile stresses in the inclusions as well as a local rotation of the principal stresses in the soil at the interfaces. As shown by finite element studies,[4] the effect of this local rotation of principal stresses on the state of stress in the reinforced soil triaxial specimen is relatively small and is therefore neglected in this analysis.

Similar mechanism of soil–reinforcement interaction develops in a reinforced soil sample when subjected to direct shearing.[8, 10] As the reinforced sand sample is being sheared in the direct (or simple) shear test, the dense sand tends to dilate. The friction mobilized at the interfaces restrains any relative displacement between the soil and the reinforcements. Consequently, the soil dilatancy is governed by the extensibility of the reinforcements. This soil–reinforcement interaction is highly dependent upon the inclination of the reinforcements with respect to the failure surface.

Different approaches have been proposed to simulate this soil–reinforcement interaction. A variety of interface elements can be used in finite element analysis based on different assumptions such as perfect adherence,[18, 19] sliding along a preferential failure plane,[20] etc. A detailed discussion of these various concepts is beyond the scope of this analysis. In this study, it is assumed that perfect adherence exists between the soil and the reinforcements. This apparently restrictive assumption was verified experimentally by Jewell[8] and Dyer and Milligan.[10] They performed direct shear tests on Leighton Buzzard sand reinforced with different types of steel grids and used X-ray radiographic technique to measure the displacement field in the soil around the grid. The results of their tests and analyses illustrate that the increase of tension forces in the reinforcement

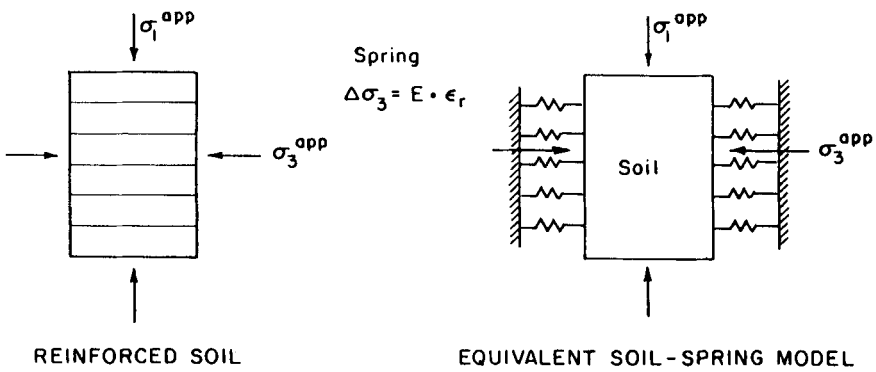

Fig. 3(a)

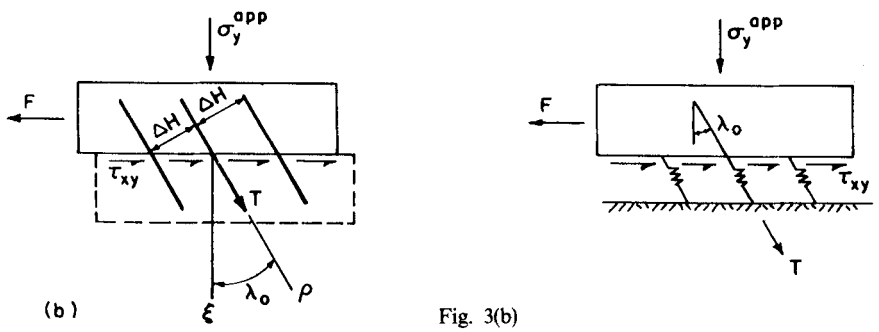

Fig. 3(b)

Figure 3. Equivalent soil–spring model of reinforced soil specimens: (a) triaxial test; (b) direct shear test

can be reasonably related to the measured extension rate of the sand in the direction of the inclusion assuming a perfect soil–inclusion adherence.

As the effect of local soil–reinforcement friction on the state of stress in the soil is neglected, the 'internal' reinforcements can be conceptually replaced by a series of elasto-plastic 'external' springs. This is schematically illustrated for both cases of triaxial (Figure 3a) and direct shear (Figure 3b) tests.

NUMERICAL SIMULATIONS OF TRIAXIAL TESTS ON REINFORCED SOIL SAMPLES

In the triaxial reinforced sand sample, the effect of the reinforcement is equivalent to an apparent increase of the radial confining pressure $\Delta\sigma_3$. This reinforcement effect, simulated using the equivalent 'external' springs concept, is mainly a function of the elastic modulus of the reinforcement (or the equivalent spring coefficient), the vertical spacing between the reinforcements, and the dilatancy properties of the compacted sand. The proposed load transfer model is used incrementally to calculate for each axial strain increment $d\varepsilon_1$:

(1) The strain and stress increments in the reinforcements

$$d\varepsilon_R = d\varepsilon_3 = \frac{\eta - 1}{\eta + 2} d\varepsilon_1; \quad d\sigma_R = E\, d\varepsilon_R \tag{8}$$

in which the dilatancy rate η is calculated from equation (8).

(2) The equivalent state of stress applied on the sand, as

$$\sigma_1 = \sigma_1^{app} \qquad \text{and } \sigma_3 = \sigma_3^{app} + \Delta\sigma_3$$

$$\Delta\sigma_3 = \sigma_R(e/S_v) \qquad \text{and } \sigma_1 = \frac{1 + h(\gamma)}{1 - h(\gamma)} \sigma_3 \tag{9}$$

in which e is the thickness of the reinforcement, S_v is the vertical spacing, and σ_1^{app} and σ_3^{app} are the axial and lateral stresses applied on the reinforced soil samples.

To verify the load transfer model, numerical test simulations are compared with the experimental results of triaxial tests performed by Long and co-workers[1] on samples of Fontainbleau sand reinforced with 18 μm thick aluminium discs. The triaxial specimen of reinforced sand (diameter 10 cm and height 20 cm) prepared by Long and co-workers had the following characteristics: *reinforcement* made of aluminium discs: elastic modulus $E = 8 \times 10^4$ MPa; tensile strength $R_T = 360$ MPa; failure strain $\varepsilon_f = 2{\cdot}4$ per cent; thickness $e = 18$ μm; and spacing $S_v = 2$ cm.

Soil. The mechanical characteristics are obtained from the analysis of the results of consolidated drained triaxial tests on unreinforced sand performed by Habib and Luang.[21] Figures 4(a) and 4(b) show the stress ratio–shear strain curves $[t/s = h(\gamma)]$ and the volumetric strain–shear strain curves $[\varepsilon_v = f(\gamma)]$ obtained under confining pressures of $\sigma_0 = 100$, 300 and 600 kPa. They illustrate the effect of the confining pressure on the peak shear strength characteristics of the sand and on the volume change properties. Figure 4(c) shows that in spite of the significant differences in volume changes measured in these three tests, the confining pressure has a rather small effect on the stress ratio–dilatancy relationship $\eta(t/s)$ which can be approximately represented by a bilinear curve with a dilatancy modulus μ_2, and a contractancy modulus μ_1. The experimental curves are compared

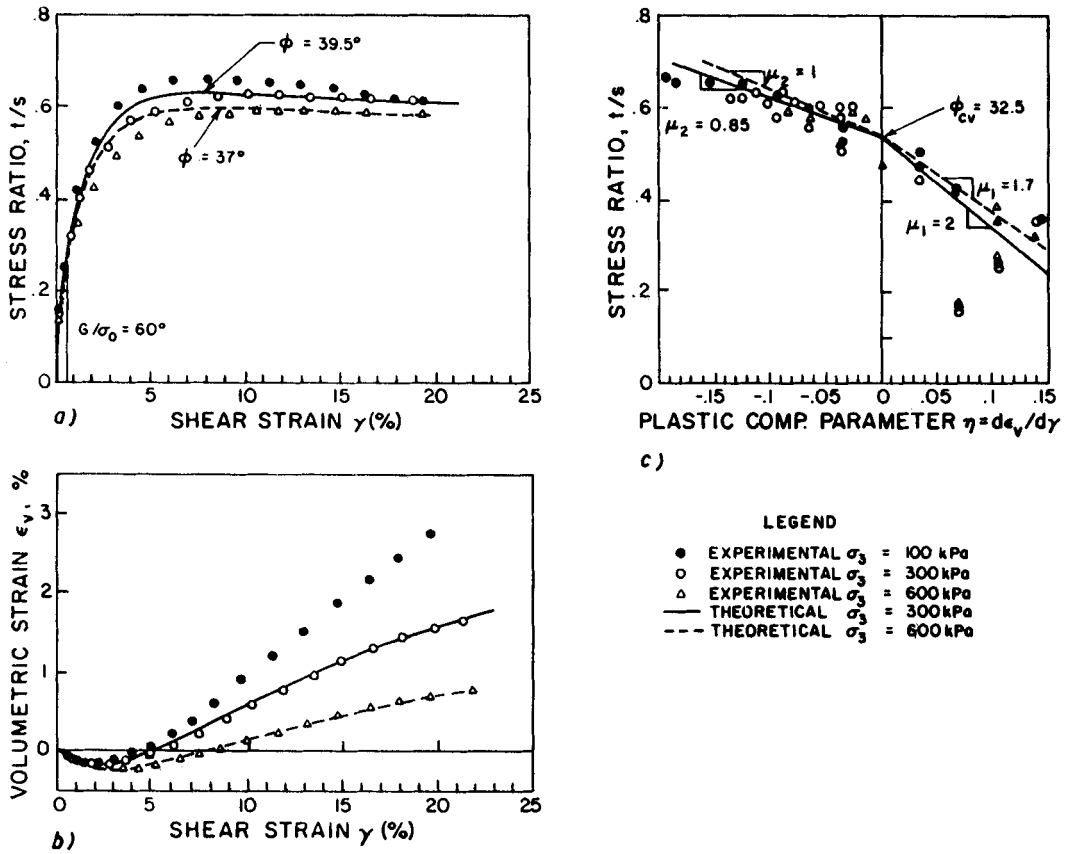

Figure 4. Modelling the behaviour of Fontainbleau sand in a triaxial test

with numerical test simulations considering, respectively:

$$\text{for } \sigma_0 = 300 \text{ kPa} \rightarrow G/\sigma_0 = 60,\ \phi = 39{\cdot}5^\circ,\ \phi_{cv} = 32{\cdot}5^\circ,\ \mu_1 = 2,\ \mu_2 = 0{\cdot}85$$

$$\text{for } \sigma_0 = 600 \text{ kPa} \rightarrow G/\sigma_0 = 60,\ \phi = 37^\circ,\ \phi_{cv} = 32{\cdot}5^\circ,\ \mu_1 = 1{\cdot}7,\ \mu_2 = 1{\cdot}0$$

As shown in Figure 4, the model predictions agree fairly well with the experimental results. For the sake of analysis, the following average soil properties are considered:

$$G/\sigma_0 = 60,\ \phi = 38{\cdot}5^\circ,\ \phi_{cv} = 32{\cdot}5^\circ,\ \mu_1 = 1{\cdot}8 \text{ and } \mu_2 = 0{\cdot}9$$

Figures 5(a) and 5(b) show the stress–strain curves obtained from triaxial tests on reinforced soil samples (diameter 10 cm, height 20 cm) performed by Long and co-workers, under $\sigma_0 = 280$ kPa and 690 kPa. The numerical test simulations using the above specified characteristics agree fairly well with the experimental curves. In particular, in the case of the test on the reinforced sand sample performed under $\sigma_0 = 280$ kPa, the sand is subjected to an equivalent confining pressure varying within the range of $280 < \sigma_3 < 600$ kPa. The shear strength characteristics used in the numerical test simulation ($\phi = 38{\cdot}5^\circ$) are representative of the sand behaviour in this range. However, in the

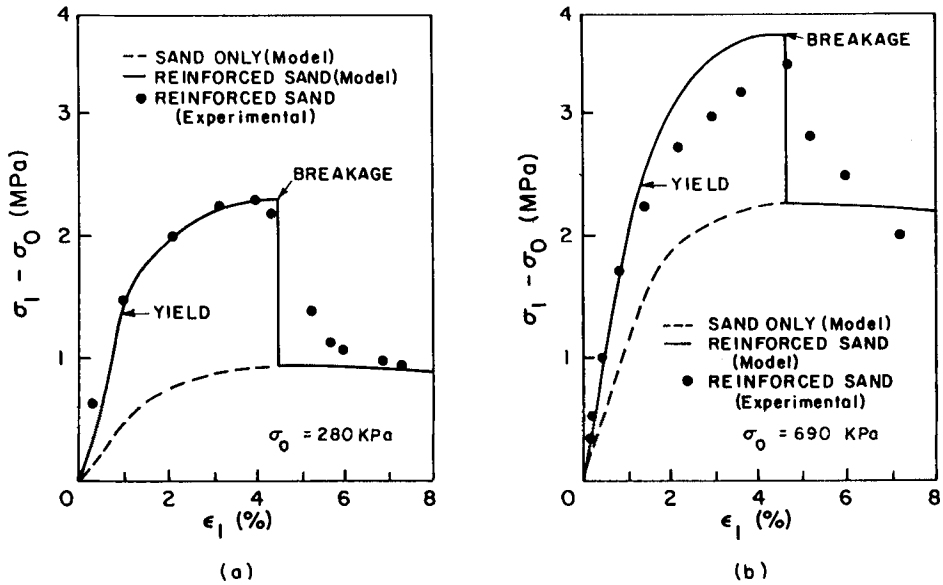

Figure 5. Numerical simulations of triaxial tests on Fontainbleau sand reinforced by aluminium foils—comparison with experimental results reported by Long *et al.*[1]

case of the test performed under $\sigma_0 = 690$ kPa, the equivalent confining pressure applied on the sand is varying within the range of $700 < \sigma_3 < 1000$ kPa. Therefore, the assumed ϕ value is overestimated, and it leads to an overestimation of the available strength of the sand. A more rational modelling approach should integrate the variation of the shear strength characteristics of the soil with the applied confining pressure.

These numerical test simulations show that the reinforcements do not modify significantly the volumetric strain of the sand during the test, but increase its resistance to the applied constant rate axial displacement. As the reinforcements reach their elastic limit they undergo plastic strains, but the axial stress applied on the reinforced earth sample is still continuously increasing until either the peak shear resistance of the sand is entirely mobilized or the reinforcements reach their failure strain. The experimental results showed that as failure occurred by breakage of the reinforcements, the shear resistance of the soil was entirely mobilized, and therefore as illustrated in Figure 6, the observed and calculated failure envelopes of the reinforced and unreinforced sands are practically parallel.

These experimental results led Long and co-workers[1] to suggest that the failure criterion of the composite reinforced soil material can be defined considering a 'pseudo' cohesion which is a function of the intrinsic soil properties, tension resistance of the inclusion and their spacing, and an equivalent friction angle which is equal to that of the unreinforced sand. However, it should be indicated that at the shearing resistance of the soil mobilized at failure by breakage of the reinforcement depends upon their extensibility or ductility. Figure 5(b) illustrates the failure curve of the reinforced soil material, assuming that the breakage occurs as the elastic limit of the reinforcement is attained (i.e. failure strain ε_f = yield strain ε_y). It shows that with quasi-inextensible, brittle reinforcements the failure shear strain of the reinforced soil material is significantly lower than the peak shear strain of the unreinforced sand. Consequently, at failure, the shear resistance of the soil is not entirely mobilized and the equivalent friction angle of the

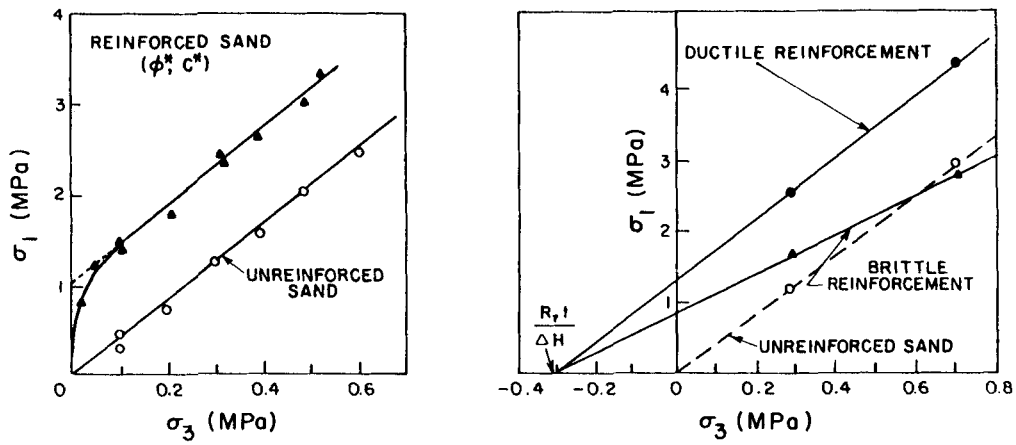

Figure 6. Failure envelopes of reinforced and unreinforced sands: (a) experimental results (Long *et al.*[1]); (b) numerical test simulations

reinforced sand is significantly smaller than that of the unreinforced sand. As a result, the reinforcing effect decreases as the applied confining pressure increases. This analysis suggests that the 'pseudo' cohesion concept cannot be used to define the failure criterion of the reinforced soil material with quasi-inextensible, brittle reinforcements.

EFFECT OF THE EXTENSIBILITY OF THE REINFORCEMENTS AND DILATANCY PROPERTIES OF THE SOIL

Figure 7 shows the effect of the elastic modulus of the reinforcements on tension forces generated in the reinforcements and on the stress–strain curve of the reinforced soil material (failure strain of the reinforcement is assumed to be infinite and no breakage can occur). As the elastic modulus of the reinforcements decreases and their extensibility increases, the efficiency of the reinforcements decreases and the peak resistance of the reinforced sand approaches that of the unreinforced sand. These theoretical results are consistent with experimental results reported by McGown and co-workers.[7] They indicated that ideally extensible inclusions ($E/E_{soil} < 3000$) do not contribute significantly to the strength of the soil, but provide greater ductility and smaller loss of post-peak strength as compared with quasi-inextensible reinforcements.

Figure 8 shows that the dilatancy properties of the sand (μ_1 and μ_2) have no significant effect on either the tension forces generated in the inclusions or the stress–strain curve of the reinforced sand triaxial sample. The results obtained with the characteristics of the Fontainbleau sand are compared with those obtained considering an incompressible sand ($\mu_1 = \mu_2 = 1000$). Note that during initial shearing as the sand contracts, the more incompressible the sand is, the larger are the tension forces generated in the inclusions and consequently the higher is the resistance of the reinforced soil to the applied axial displacement. The effect of soil contractancy (or dilatancy) on tension forces generated in the inclusions depends upon their extensibility. Also, the higher the elastic modulus of the reinforcements is, the larger is the effect of the contractancy of the soil on the stress–strain relationship of the reinforced soil. With quasi-inextensible reinforcements, the elastic limit is attained when the soil is still contracting. When the yield stress of the reinforcements is attained, the equivalent confining pressure applied on the reinforced soil sample reaches a constant

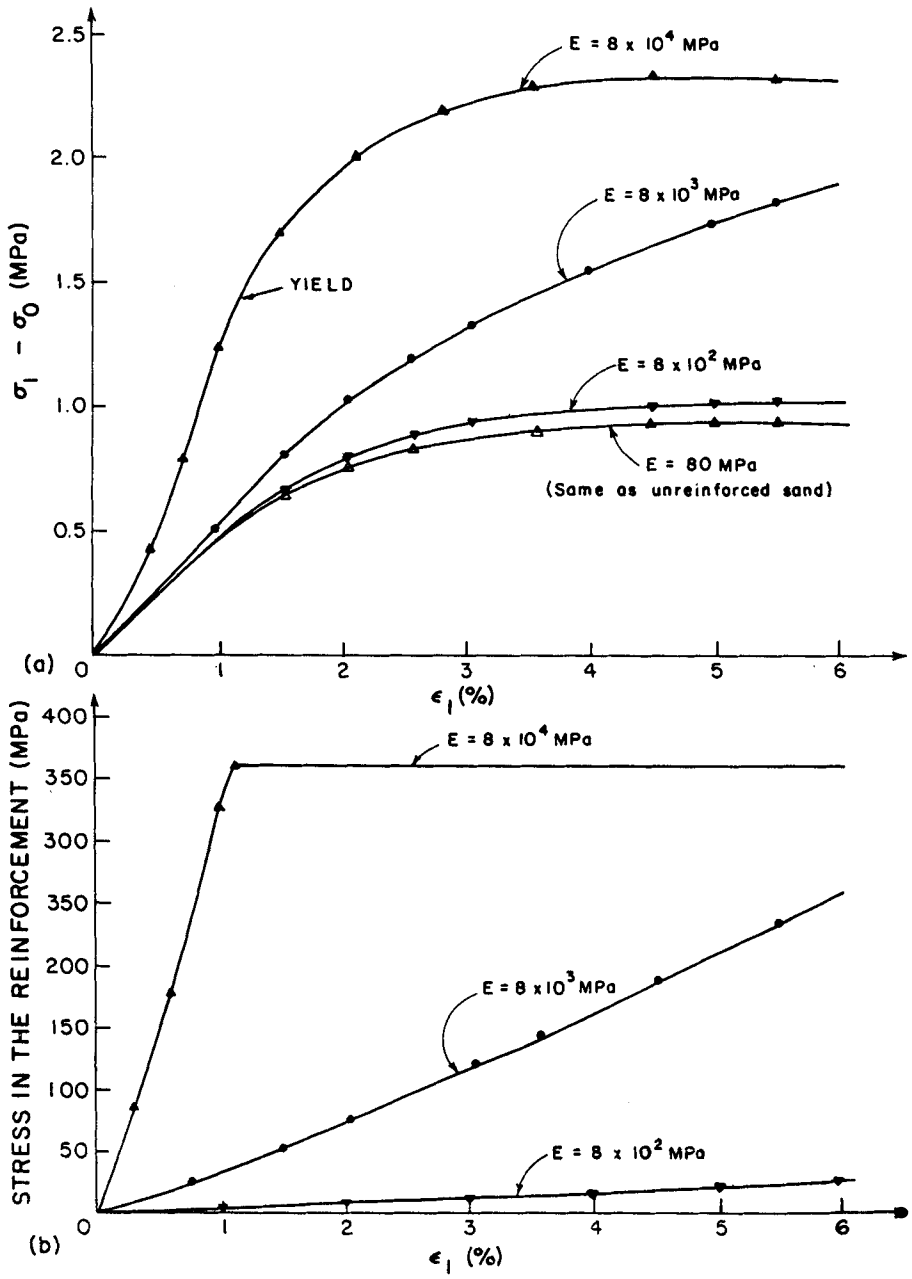

Figure 7. Effect of the extensibility of the reinforcement on: (a) shear curve; (b) forces generated in the inclusions

value of $\sigma_3 = \sigma_3^{app} + R_T \cdot e/S_v$, and the stress–strain curve of the reinforced sand approaches that of an unreinforced sand under the same constant equivalent confining pressure. With more extensible reinforcements, larger axial and radial displacements are required to effectively mobilize tension forces. However, soil dilatancy does not seem to have any significant effect on the response of the reinforced soil material to a triaxial compression.

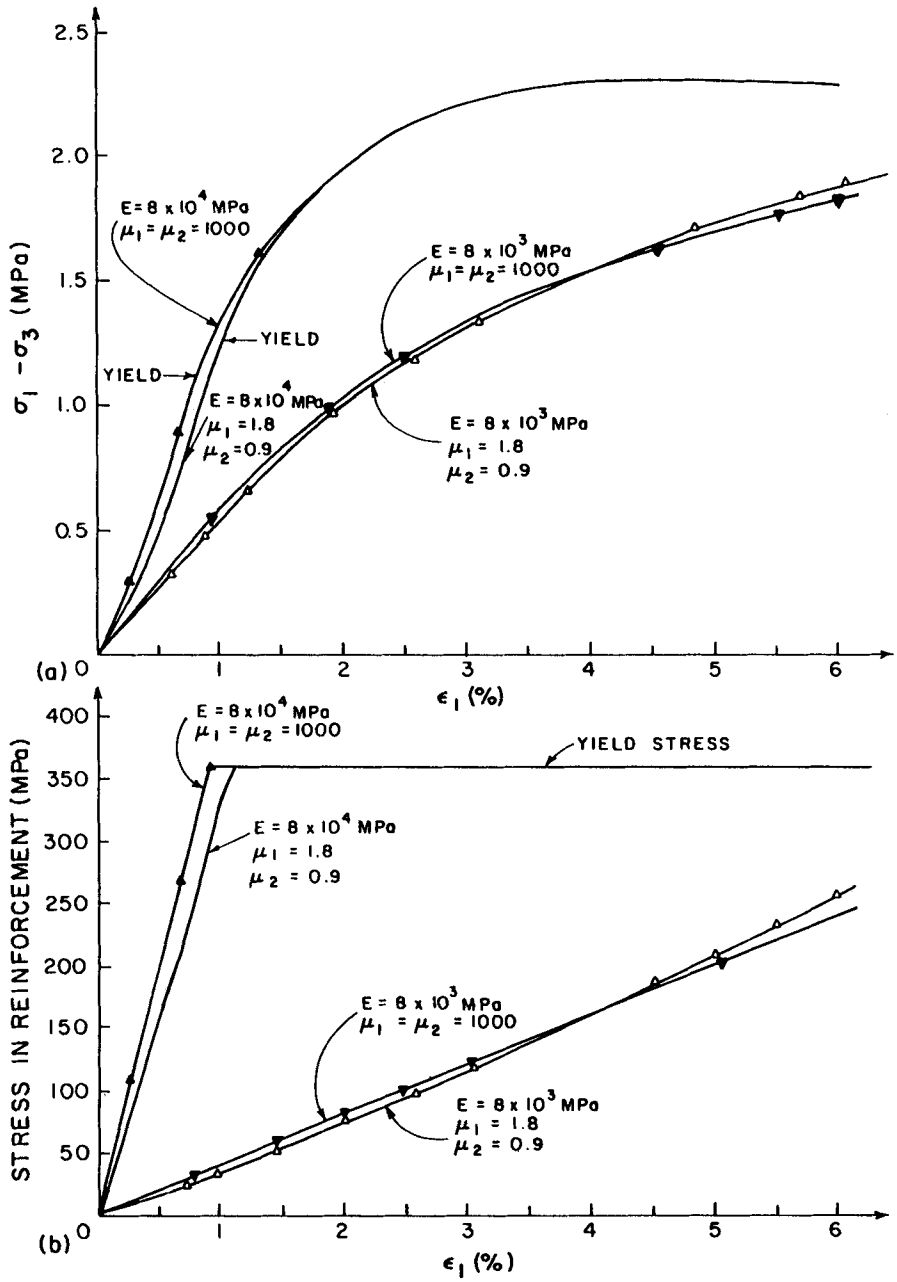

Figure 8. Effect of the dilatance of the soil on: (a) shear curve; (b) tension forces generated in the inclusions

CONCLUSIONS

A load transfer model is proposed to predict forces generated in inclusions of reinforced soils assuming a perfect soil–inclusion adherence and an elasto-plastic, strain hardening behaviour of the soil. Comparison of numerical simulations and experimental results of triaxial tests on sand

samples reinforced by aluminium discs suggests that the model can be adequately used to analyse the response of the reinforced soil material to loading. In particular, it allows an evaluation of the effect of soil dilatancy (or contractancy) on tension forces generated in inclusions during shearing and to integrate in analysis/design nonlinear stress–strain relationships of the reinforcements. The numerical test simulation indicate that:

1. The reinforcements do not modify significantly the volumetric strain of the sand during shearing, but increase its resistance to the applied constant rate axial displacement.
2. The more inextensible the reinforcement is, the more significant its strengthening effect will be. Extensible reinforcements do not contribute significantly to the shear resistance of the reinforced soil, but they increase its ductility.
3. In the case of quasi-inextensible reinforcements, the elastic limit is attained when the soil is still contracting. The less compressible the soil is, the larger are the tension forces generated in the inclusions and the higher is the resistance of the reinforced soil to the applied axial displacement.
4. Soil contractancy (or dilatancy) does not seem to have a significant effect on the response of reinforced soil to a triaxial compression. Numerical simulations of direct shear tests on reinforced soil samples discussed by the authors in the companion paper indicate that the effect of the contractancy/dilatancy properties of the soil is highly dependent on the applied stress path.
5. The global shear resistance of the reinforced soil material depends upon: (a) the limit tension (or compression) forces in the inclusions, which is equal to either the tensile strength or the pull-out resistance, and (b) the shearing resistance of the soil mobilized at failure of the inclusion. At failure by breakage of the inclusions, the mobilized shearing resistance of the soil depends upon the extensibility/ductility of the reinforcements. With quasi-inextensible, brittle reinforcements the failure shear strain of the reinforced soil material can be significantly lower than the peak shear strain of the unreinforced sand and the mobilized shearing resistance of the soil can therefore be significantly reduced.

The proposed soil model, at this time, has been verified with respect to only two loading paths—triaxial compression and direct shearing. These loading paths are of a specific interest for the analysis and design of reinforced soil retaining structures. For these stress paths, it may be appropriate to use γ as the hardening parameter. However, for general modelling and other paths, it is more appropriate to use internal variables such as trajectory of plastic strains.

ACKNOWLEDGEMENTS

The authors wish to thank the Department of Civil Engineering, Louisiana State University, for supporting this study and particularly Ms. Susan Sartwell for her help in preparing this manuscript.

REFERENCES

1. N. T. Long, Y. Guegan and G. Legeay, 'Etude de la terre armee a l'appareil triaxial', *Rapport de Recherche No.17*, Laboratoire Central des Ponts et Chaussees, Paris, France (1972).
2. J. Bacot, 'Contribution a l'etude du frottement entre une inclusion souple et un materiau pulverulent, cas de la terre armee,' *These de Doctorat d'etat*, Lyon (1981).
3. M. R. Hausmann, 'Strength of reinforced earth', Proc. of ARRB, Vol. 8, 1976.
4. Z. Yang, 'Strength and deformation characteristics of reinforced sand', *Ph.D. thesis*, UCLA (1973).

5. B. B. Broms, 'Polyester fabric as reinforcement in soil', Proc. Int. Conf. on Use of Fabrics in Geotechnics, Vol. 1, 1977, pp. 129–135.
6. A. McGown and K. Z. Andrawes, 'The influence of non-woven fabric inclusions on the stress strain behavior of a soil mass', Proc. Int. Conf. on Use of Fabrics in Geotechnics, Vol. 1, 1977, pp. 161–165.
7. A. McGown, K. Z. Andrawes and M. M. Al Hasani, 'Effect of inclusion properties on the behavior of sand', *Geotechnique*, No. 3 (1978).
8. R. A. Jewell, 'Some effects of reinforcement on the mechanical behavior of soils', *Ph.D. thesis*, Univ. of Cambridge (1980).
9. D. H. Gray and H. Ohashi, 'Mechanics of fiber reinforcement in sand', *J. Geotech. Eng. Div., A.S.C.E.*, **109** (GT3), 335–353 (1983).
10. N. R. Dyer and G. W. E. Milligan, 'A photoelastic investigation of the interaction of a cohesionless soil with reinforcement placed at different orientations', Proc. Int. Conf. on Insitu Soil and Rock Reinforcement, Session 2, 1984, pp. 257–262.
11. D. H. Gray and T. Al Refeai, 'Behavior of fabric versus fiber reinforced sand', *J. Geotech. Eng. Div., A.S.C.E.*, **112**(8), 804–820 (1986).
12. A. Guermazi, 'Etude theorique et experimentale du comportement d'un sol renforce par colonnes ballastees', *Ph.D. thesis*, Univ. of Paris VI, CERMES-ENPC, France (1986).
13. C. P. Wroth, 'The behavior of soil and other granular media when subject to shear', *Ph.D. thesis*, Univ. of Cambridge (1958).
14. H. B. Poorooshasb, 'The properties of soil and other granular media in simple shear', *Ph.D. thesis*, Univ. of Cambridge (1961).
15. M. A. Stroud, 'The behavior of sand at low stress levels in the simple shear apparatus', *Ph.D. thesis*, Univ. of Cambridge (1971).
16. I. A. A. Smith, 'Stress and strain in sand mass adjacent to a model wall', *Ph.D. thesis*, Univ. of Cambridge (1972).
17. H. Vidal, 'La terre armee's', *Annales de l'Institut Technique des Batiments et des Travaux Publiques*, Paris, pp. 888–938 (July–Aug. 1966).
18. L. R. Herrmann and Z. El Yassin, 'Numerical analysis of reinforced soil systems', Proc. Symp. on Earth Reinforcement, ASCE Annual Convention, Pittsburgh, 1978, pp. 428–457.
19. C. K. Shen, S. Bang and L. R. Herrmann, 'Ground movement analysis of an earth support system', *J. Geotech. Eng. Div., A.S.C.E.*, **107**(GT12), 1625–1642 (1981).
20. I. Juran, S. Shafiee and F. Schlosser, 'Numerical study of nailed soil retaining structures', Proc. 11th Conf. on Soil Mechanics and Foundation Engineering, Vol. 3, San Francisco, 1985, pp. 1713–1716.
21. P. Habib and M. P. Luong, 'Sols pulverulents sous chargements cycliques', Seminaire Materiaux et Structures Sous Chargements Cycliques, Ecole Polytechnique, France (1979).